Acta Crystallographica Section F
Structural Biology and Crystallization Communications
ISSN 1744-3091

Preliminary crystallographic analysis of two oligomerization-deficient mutants of the aerolysin toxin, H132D and H132N, in their proteolyzed forms

Lucile Pernot,[a]*‡ Marc Schiltz[b] and F. Gisou van der Goot[a]

[a]Global Health Institute, Ecole Polytechnique Fédérale de Lausanne, Faculty of Life Sciences, Station 15, CH-1015 Lausanne, Switzerland, and [b]Laboratoire de Cristallographie, Ecole Polytechnique Fédérale de Lausanne, CH-1015 Lausanne, Switzerland

‡ Present address: Section des Sciences Pharmaceutiques, Université de Genève, Université de Lausanne, Biochimie Pharmaceutique, Quai Ernest Ansermet 30, CH-1211 Genève 4, Switzerland.

Correspondence e-mail: lucile.pernot@unige.ch

Received 26 June 2010
Accepted 12 October 2010

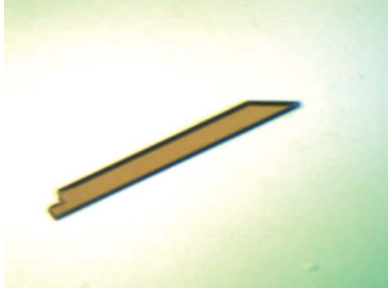

Aerolysin is a major virulence factor produced by the Gram-negative bacterium *Aeromonas hydrophila* and is a member of the β-pore-forming toxin family. Two oligomerization-deficient aerolysin mutants, H132D and H132N, have been overproduced, proteolyzed by trypsin digestion and purified. Crystals were grown from the proteolyzed forms and diffraction data were collected for the two mutants to 2.1 and 2.3 Å resolution, respectively. The prism-shaped crystals belonged to space group *C*2. The crystal structure of the mutants in the mature, but not heptameric, aerolysin form will provide insight into the intermediate states in the oligomerization process of a pore-forming toxin.

1. Introduction

Aerolysin is a major virulence factor produced by the Gram-negative bacterium *Aeromonas hydrophila*, which induces gastrointestinal infections with diarrhoea as well as deep-wound infections in humans (Abrami *et al.*, 2000; Aroian & van der Goot, 2007). It belongs to the largest group of well characterized bacterial toxins, *i.e.* the β-pore-forming toxins (Iacovache *et al.*, 2008, 2010; Parker & Feil, 2005). The toxin is secreted by the bacterium into the extracellular medium *via* a type II secretion system as proaerolysin, an inactive water-soluble precursor of 470 amino acids. The structure of proaerolysin as a dimer, which has been solved by X-ray crystallography to a resolution of 2.8 Å (PDB entry 1pre; Parker *et al.*, 1994), reveals that it is an L-shaped molecule formed by a small N-terminal domain and an elongated lobe divided into three structural domains. Proaerolysin interacts with target cells by binding specifically to glycosylphosphatidylinositol-anchored proteins (GPI-APs) that act as receptors (Fivaz *et al.*, 2001). The toxin binds to its receptor *via* two distinct binding sites: to the glycan core of the GPI anchor and to the N-linked sugar of the protein moiety of the receptor (Hong *et al.*, 2002; Diep *et al.*, 1998).

Proaerolysin is processed into an activated form, aerolysin, following proteolysis in the C-terminal extremity of the protein between residues 420 and 430 encompassing the cleavage site (van der Goot *et al.*, 1992). This proteolysis can be achieved by proteases produced either by the bacterium itself, enzymes of the digestive tract such as trypsin or chymotrypsin, or by cell-surface-associated proteases such as furin (Abrami *et al.*, 1998; Howard & Buckley, 1985). Previous studies using proaerolysin point mutants and fluorescence energy transfer indicated that a carboxy-terminal propeptide (CTP) composed of 43 residues is released from the body of the toxin and does not participate in subsequent formation of the transmembrane channel (van der Goot *et al.*, 1994). However, biochemical studies on the related toxin *Clostridium septicum* α-toxin indicated that the CTP remains bound to the mature protein and is only displaced during the oligomerization process (Sellman & Tweten, 1997).

Mature aerolysin oligomerizes into a ring-like heptamer (Wilmsen *et al.*, 1991; Moniatte *et al.*, 1996). During heptamerization, all of the

monomers bring together an amphipathic β-hairpin to form a β-barrel, the exterior of which is hydrophobic. Owing to the exposure of hydrophobic regions, the aerolysin heptamer then spontaneously inserts into the lipid bilayer of the membrane to create a transmembrane channel. Heptamerization requires a high local toxin concentration, which is achieved by binding to receptors on the cell surface and subsequent localization in specific membrane domains (Abrami & van der Goot, 1999).

The histidine residue at position 132 located in domain 2 has been shown to be essential in the initiation of oligomerization. Indeed, substitution of His132 by an asparagine or an aspartate prevents oligomerization of the toxin (Green & Buckley, 1990; Wilmsen *et al.*, 1991; Cabiaux *et al.*, 1997). Further investigations confirmed that the protonation state of His132 is crucial for oligomerization to occur (Buckley *et al.*, 1995).

Membrane insertion of aerolysin leads to permeabilization of the plasma membrane and ultimately induces the death of target cells (Gurcel *et al.*, 2006). In domain 3 of the toxin, we identified a loop that contains an alternating pattern of charged and uncharged residues lining the transmembrane channel (Iacovache *et al.*, 2006; Rossjohn *et al.*, 1998). The tip of this loop is composed of a stretch of five hydrophobic residues. We have shown that this hydrophobic turn drives membrane insertion and, once it has crossed the membrane, folds in a rivet-like fashion (Iacovache *et al.*, 2006). These recent findings challenge a previously proposed model in which domain 4 lines the channel and raise the possibility that this domain undergoes a major conformational change upon proteolytic activation of the precursor and/or heptamerization.

While the structure of dimeric proaerolysin is known at high resolution (Parker *et al.*, 1994) and that of the aerolysin heptamer is known at low (13 Å) resolution (Tsitrin *et al.*, 2002), information regarding nonheptameric aerolysin is lacking. Structural studies are hampered by the fact that this species is transient, especially at the high concentrations that would be required to induce crystallization. To circumvent this difficulty, we decided to take advantage of the fact that the two mutants H132N and H132D are oligomerization-deficient in order to gain access to the activated aerolysin structure, possibly in its monomeric state. Here, we report the purification, crystallization and preliminary X-ray data analysis of the oligomerization-deficient mutants H132N and H132D in their proteolyzed forms. This is the first time that an intermediate in the oligomerization process of pore-forming toxins has been studied by X-ray crystallography and the outcome should provide insight into the changes that prime the toxin for oligomerization.

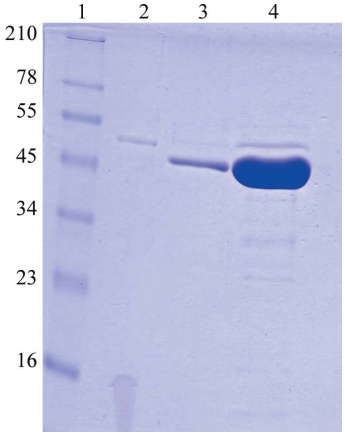

Figure 1
12% SDS–PAGE analysis of trypsin proteolysis of the aerolysin mutant H132N. Lane 1, molecular-mass markers (sizes are indicated in kDa). Lane 2, H132N before proteolysis. Lane 3, proteolyzed H132N after trypsin proteolysis. Lane 4, after addition of the trypsin inhibitor and overnight dialysis at 277 K: the proteolyzed H132N was concentrated before loading onto the gel-filtration column.

2. Experimental procedure

2.1. Plasmid preparation and protein overproduction and purification

The pET22b(+):aerA plasmid expressing wild-type proaerolysin from residue Ala1 to residue Gln470 with a tail of six histidine residues at the C-terminus was used as a starting matrix DNA (Iacovache *et al.*, 2006). Site-directed mutagenesis was performed using the QuikChange Kit (Stratagene). The primer 5′-TGG GTG GGC GGC AAT *GAC* AGC CAA TAT GTC GGC-3′ and its reverse complement were used to create the pET22b(+):aerA-H132D plasmid. The introduction of the expected mutation was confirmed by DNA sequencing. The pET22b(+):aerA-H132N plasmid had previously been prepared. *Escherichia coli* strain BL21 (DE3) was transformed separately with the two plasmids in order to overproduce the two

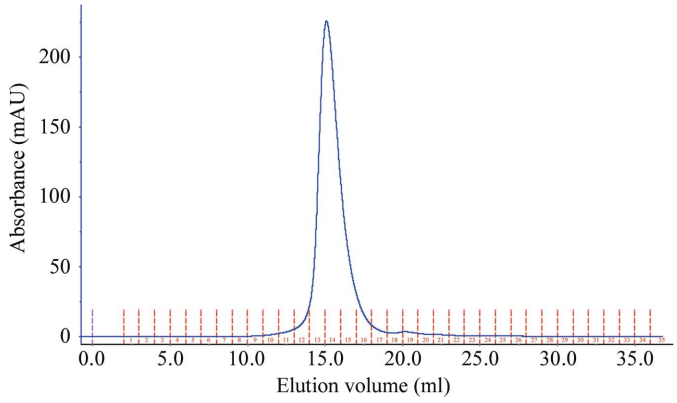

Figure 2
Gel-filtration chromatogram of the proteolysed mutant H132N.

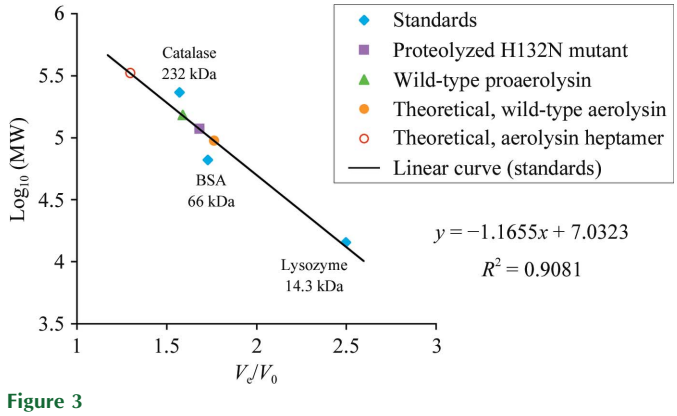

Figure 3
Determination of the expected association state of the proteolyzed H132N mutant. The calibration curve of the gel-filtration column was produced using blue dextran (used to determined a void volume of V_0 = 8.9 ml); catalase (232 kDa), BSA (66 kDa) and lysozyme (14.3 kDa) were used as standards (blue diamonds). The elution volumes (V_e) of the proteolyzed H132N mutant (magenta square) and wild-type proaerolysin (green triangle) were expressed as relative values (V_e/V_0) and are reported on the graph. Both samples were injected four times. Using their theoretical molecular masses, the aerolysin wild-type dimer (94.8 kDa; orange filled circle) and the aerolysin heptamer (331.8 kDa; red circle) are reported on the graph for comparison.

point mutants in the periplasmic compartment of the bacteria as C-terminally His-tagged proteins.

For both mutants, the same protocol was applied for overproduction and purification. One isolated colony was picked and allowed to grow in Luria–Bertani medium supplemented with ampicillin (100 µg ml^{-1}) at 310 K under 220 rev min^{-1} agitation. The saturated overnight culture was diluted in fresh LB medium and grown for 2.5 h at 310 K with shaking. Protein overproduction was induced by addition of 1 m*M* isopropyl *β*-D-1-thiogalactopyranoside when the culture reached an $OD_{600\,nm}$ of 0.6–0.8 and was allowed to proceed at 295–298 K for 3 h. Bacteria were harvested by centrifugation at 4000 rev min^{-1}. In order to release the periplasmic fraction by osmotic shock, the pelleted bacteria were resuspended in a sucrose shock solution consisting of 20 m*M* Tris–HCl pH 8, 5 m*M* EDTA, 20% sucrose, to which lyzozyme was added to a final concentration of 0.1 mg ml^{-1}, and left on ice for 45 min. The suspension was clarified by centrifugation at 10 000 rev min^{-1} for 15 min at 277 K and the supernatant was recovered and dialysed overnight at 277 K against a buffer consisting of 20 m*M* sodium phosphate pH 7.4, 0.5 *M* NaCl. The recovered fraction was then loaded onto a Sepharose nickel-affinity chromatography column. The mutant was eluted using a gradient with an increasing proportion of a buffer containing 20 m*M* sodium phosphate pH 7.4, 0.5 *M* NaCl and 0.5 *M* imidazole. The mutant eluted at 55% of the gradient.

The eluted fraction containing the protein was dialysed overnight at 277 K in a buffer consisting of 20 m*M* Tris–HCl pH 8, 150 m*M* NaCl. Once recovered, the protein was brought to a concentration of 0.8 mg ml^{-1} and submitted to proteolysis. The concentration of the protein solution was determined by measuring the optical density at 280 nm, considering that a 1 mg ml^{-1} sample has an OD of 2.5 (van der Goot *et al.*, 1994). For the proteolysis step, soluble trypsin at 1 mg ml^{-1} was added to the protein solution at a mass ratio of 1:400. The digestion was performed at room temperature for 45 min. The proteolysis reaction was stopped by adding a trypsin–chymotrypsin inhibitor to the mixture to a concentration of 10 mg ml^{-1} and incubating for 30 min at room temperature. The digested protein was then dialyzed overnight at 277 K in the buffer (20 m*M* HEPES pH 7.4, 150 m*M* NaCl) usually used for oligomerization of the toxin.

At each step, a small amount of the sample was picked up and loaded onto an SDS–polyacrylamide gel to check whether the heptamer was formed. Indeed, formation of the aerolysin heptamer can be monitored by an SDS–PAGE analysis run under denaturing conditions because aerolysin heptamers are very stable and can withstand boiling in the sample buffer containing sodium dodecyl sulfate and the reducing agent *β*-mercaptoethanol (Garland & Buckley, 1988; Lesieur *et al.*, 1999; Tsitrin *et al.*, 2002). Under denaturing conditions, the aerolysin heptamer migrates in the gel with an apparent molecular mass of 333 kDa (Garland & Buckley, 1988;

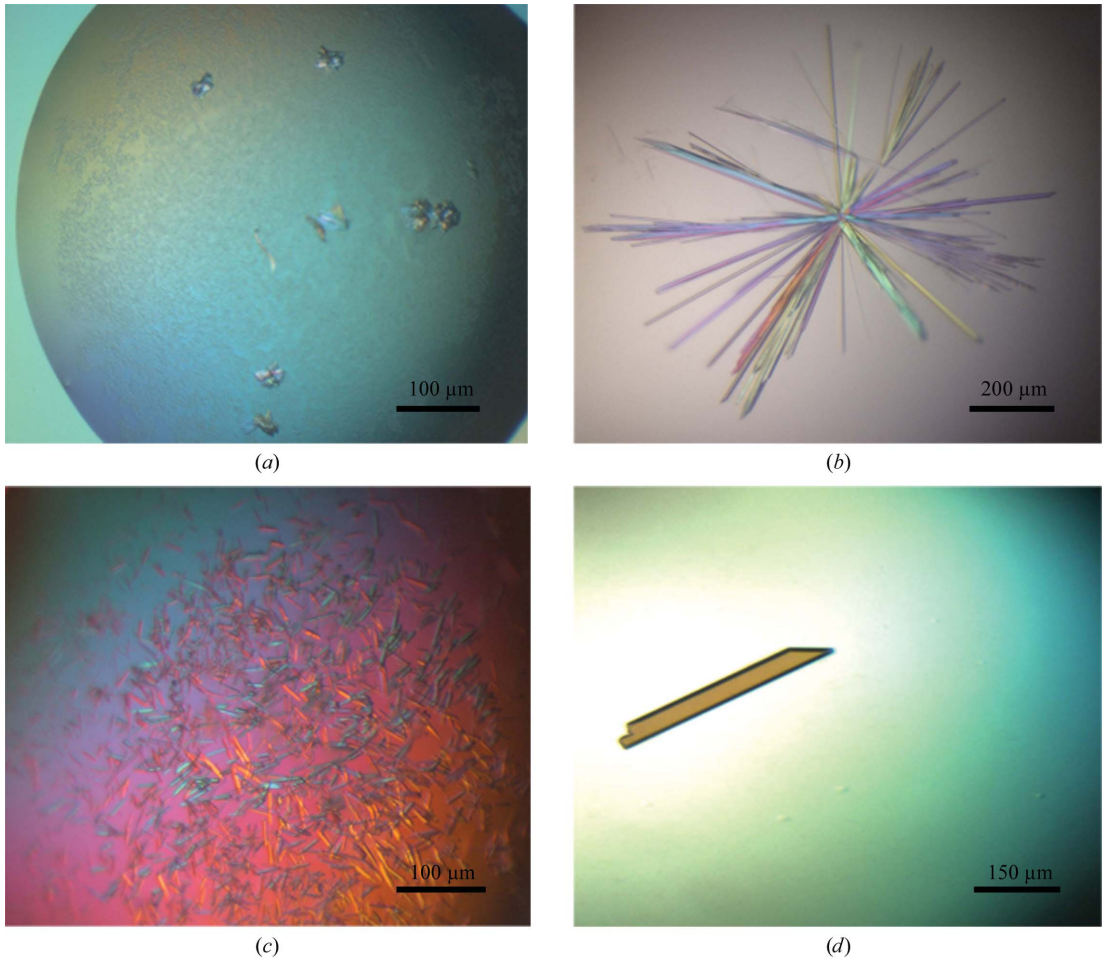

Figure 4
Crystallization trials for the H132N and H132D mutants. (*a*) One single hit was found for H132N with the condition 35%(*v*/*v*) 5/4 PO/OH, 50 m*M* HEPES pH 7.5, 0.2 *M* KCl. (*b*) The same crystallization condition with a different buffer, 50 m*M* sodium acetate pH 5.4, was tested with H132D and sea urchin-like crystals appeared. (*c*) The removal of KCl allowed single crystals of H132D to appear. (*d*) Final crystallization condition for H132D: 19%(*v*/*v*) 5/4 PO/OH, 50 m*M* sodium acetate pH 5.4.

Lesieur *et al.*, 1999) and the corresponding band usually appears at the top of the gel. The digestion of the mutant was complete and the oligomerization following activation did not occur (Fig. 1). The proteolyzed protein was further purified by gel filtration, each time loading about 0.5 ml at a concentration of 5 mg ml^{-1} onto a Superdex 200 10/300 GL column (GE Healthcare) running at 0.5 ml min^{-1} in 20 m*M* HEPES pH 7.4, 150 m*M* NaCl. After this last step of purification, the recovered sample was homogenous and was eluted with an elution volume of 15 ml (Fig. 2), which corresponds to an apparent molecular mass of 116 kDa (Fig. 3). Taking into account that the theoretical molecular mass of the activated aerolysin wild-type dimer is 94.8 kDa, it is expected that the proteolyzed mutant H132N is associated as a dimer (Fig. 3). Finally, at the end of the last purification step by gel filtration, five 1 ml fractions containing the protein were collected and concentrated by centrifugation in a 30 kDa molecular-mass cutoff Vivaspin centrifugal concentrator (Vivascience, Sartorius Group) to a concentration of 5 mg ml^{-1} at 277 K.

2.2. Crystallization

Crystallization trials were carried out by sparse-matrix screening (Jancarik *et al.*, 1991) at 291 K using the hanging-drop vapour-diffusion technique. 2 µl drops were prepared by mixing equal volumes of protein solution and reservoir solution and were equilibrated against 500 µl reservoir solution. For the first round of crystallization trials, the proteolyzed H132N protein (5 mg ml^{-1} in 20 m*M* HEPES pH 7.4, 150 m*M* NaCl) was screened against various conditions: those in which wild-type proaerolysin crystals appeared (Parker *et al.*, 1994) and conditions from several crystallization screening kits such as Crystal Screen, Crystal Screen 2 and Index Screen (Hampton Research, USA). Precipitates appeared in most of the drops. A unique first hint was identified with condition No. 56 of Hampton Research Index Screen [35%(*v*/*v*) pentaerythritol propoxylate (5/4 PO/OH), 0.05 *M* HEPES pH 7.5, 0.2 *M* potassium chloride], in which initial crystal germs appeared after two weeks (Fig. 4*a*).

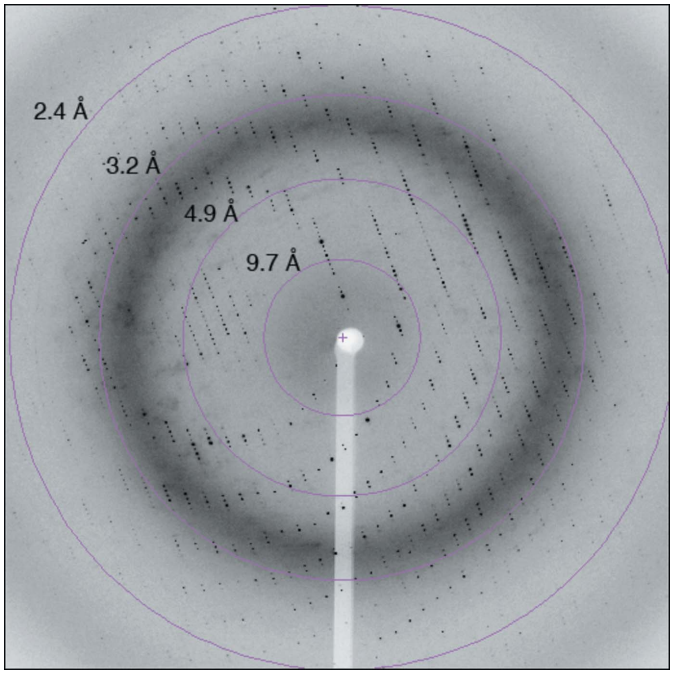

Figure 5
A diffraction image (1° rotation) recorded on the H132D aerolysin mutant crystal.

Table 1
X-ray diffraction data-collection parameters and statistics.

Values in parentheses are for the highest resolution shell.

	H132D	H132N
Space group	*C*2	*C*2
Unit-cell parameters		
a (Å)	95.72	95.98
b (Å)	70.21	69.31
c (Å)	165.44	165.23
β (°)	109.11	109.01
Resolution limits (Å)	56.0–2.1 (2.21–2.10)	56.0–2.3 (2.42–2.30)
No. of measured reflections	1270180	239594
Unique reflections	59799	43658
Completeness (%)	98.6 (97.8)	95.4 (74.7)
Multiplicity	21.2 (10.4)	5.5 (5.0)
$R_{\rm merge}$† (%)	8.8 (40.5)	7.5 (39.6)
$\langle I/\sigma(I)\rangle$	24.5 (3.1)	16.3 (3.7)

† $R_{\rm merge} = \sum_{hkl}\sum_i |I_i(hkl) - \langle I(hkl)\rangle| / \sum_{hkl}\sum_i I_i(hkl)$, where $I_i(hkl)$ represents the *i*th measurement of the intensity of the *hkl* reflection and its symmetry equivalent and $\langle I(hkl)\rangle$ is the average intensity of the *hkl* reflection.

Optimization experiments were set up manually (by testing several buffer solutions with various pH ranges and different concentrations of KCl) and were performed on the proteolyzed H132D protein (Figs. 4*b* and 4*c*). Finally, H132D crystals suitable for X-ray diffraction experiments grew within one week in 17–19% 5/4 PO/OH, 50 m*M* sodium acetate pH 5.4 (Fig. 4*d*). H132N crystals grew in a similar solution in which the concentration of 5/4 PO/OH was increased to 24–28%.

2.3. Data collection and processing

Diffraction data were recorded at 100 K. Prior to data collection, crystals were briefly immersed in a cryoprotectant solution with the same composition as the mother liquor but with an increase in the concentration of 5/4 PO/OH (to 30% for H132D crystals and 32% for H132N crystals). After this rapid immersion, the crystals were flash-cooled by plunging them into liquid nitrogen. In this case, 5/4 PO/OH could not only be used as a crystallization agent but also as a cryoprotectant (Gulick *et al.*, 2002). X-ray diffraction data sets for the two aerolysin mutants H132D and H132N were collected on beamline X06SA at the Swiss Light Source, Villigen, Switzerland equipped with a MAR CCD detector and tuned to a wavelength of 0.9536 Å. Each data set was obtained from a single crystal and more than 360° of data were recorded. A typical diffraction pattern recorded using a H132D crystal is shown in Fig. 5. Raw diffraction images were indexed and integrated with *MOSFLM* (Leslie, 2006) and scaled with *SCALA* (Evans, 2006) within the *CCP*4 program suite (Collaborative Computational Project, Number 4, 1994). Relevant statistics are given in Table 1.

3. Results and discussion

We have crystallized two oligomerization-deficient mutants of aerolysin, H132D and H132N, in their proteolyzed forms. The prism-shaped crystals of both mutants belonged to space group *C*2 and have fairly similar unit-cell parameters (a = 95.72, b = 70.21, c = 165.44 Å, β = 109.11° for H132D and a = 95.98, b = 69.31, c = 165.23 Å, β = 109.01° for H132N), suggesting that they are isomorphous. However, the crystals of the two mutants are different from the known wild-type crystal form, which belongs to space group $P4_32_12$ (Parker *et al.*, 1994). With a molecular mass of 47.4 kDa per monomer, a reasonable value of the Matthews coefficient $V_{\rm M}$ (Matthews, 1968) was obtained for two monomers in the asymmetric

unit (V_M = 2.77 Å^3 Da^{-1}). This value is in the normal range for globular proteins and corresponds to a solvent content of 56%. This analysis confirms that even at the high concentrations required for crystallization the mutants remain nonheptameric after proteolytic processing.

Attempts to solve the structures of the two proteolyzed mutants by molecular replacement are currently under way.

We thank Clemens Schulze-Briese for assistance in collecting the data on beamline X06SA of the Swiss Light Source at the Paul Scherrer Institut, Villigen, Switzerland. This work was supported by the Swiss National Science Foundation. FGvdG is an international Fellow of the Howard Hughes Medical Institute.

References

Abrami, L., Fivaz, M., Decroly, E., Seidah, N. G., Jean, F., Thomas, G., Leppla, S. H., Buckley, J. T. & van der Goot, F. G. (1998). *J. Biol. Chem.* **273**, 32656–32661.
Abrami, L., Fivaz, M. & van der Goot, F. G. (2000). *Trends Microbiol.* **8**, 168–172.
Abrami, L. & van der Goot, F. G. (1999). *J. Cell Biol.* **147**, 175–184.
Aroian, R. & van der Goot, F. G. (2007). *Curr. Opin. Microbiol.* **10**, 57–61.
Buckley, J. T., Wilmsen, H. U., Lesieur, C., Schultze, A., Pattus, F., Parker, M. W. & van der Goot, F. G. (1995). *Biochemistry*, **34**, 16450–16455.
Cabiaux, V., Buckley, J. T., Wattiez, R., Ruysschaert, J.-M., Parker, M. W. & van der Goot, F. G. (1997). *Biochemistry*, **36**, 15224–15232.
Collaborative Computational Project, Number 4 (1994). *Acta Cryst.* D**50**, 760–763.
Diep, D. B., Nelson, K. L., Raja, S. M., Pleshak, E. N. & Buckley, J. T. (1998). *J. Biol. Chem.* **273**, 2355–2360.
Evans, P. (2006). *Acta Cryst.* D**62**, 72–82.
Fivaz, M., Abrami, L., Tsitrin, Y. & van der Goot, F. G. (2001). *Toxicon*, **39**, 1637–1645.
Garland, W. J. & Buckley, J. T. (1988). *Infect. Immun.* **56**, 1249–1253.
Goot, F. G. van der, Hardie, K. R., Parker, M. W. & Buckley, J. T. (1994). *J. Biol. Chem.* **269**, 30496–30501.
Goot, F. G. van der, Lakey, J. H., Pattus, F., Kay, C. M., Sorokine, O., Van Dorsselaer, A. & Buckley, T. (1992). *Biochemistry*, **31**, 8566–8570.
Green, M. J. & Buckley, J. T. (1990). *Biochemistry*, **29**, 2177–2180.
Gulick, A. M., Horswill, A. R., Thoden, J. B., Escalante-Semerena, J. C. & Rayment, I. (2002). *Acta Cryst.* D**58**, 306–309.
Gurcel, L., Abrami, L., Girardin, S., Tschopp, J. & van der Goot, F. G. (2006). *Cell*, **126**, 1135–1145.
Hong, Y., Ohishi, K., Inoue, N., Kang, J. Y., Shime, H., Horiguchi, Y., van der Goot, F. G., Sugimoto, N. & Kinoshita, T. (2002). *EMBO J.* **21**, 5047–5056.
Howard, S. P. & Buckley, J. T. (1985). *J. Bacteriol.* **163**, 336–340.
Iacovache, I., Bischofberger, M. & van der Goot, F. G. (2010). *Curr. Opin. Struct. Biol.* **20**, 241–246.
Iacovache, I., Paumard, P., Scheib, H., Lesieur, C., Sakai, N., Matile, S., Parker, M. W. & van der Goot, F. G. (2006). *EMBO J.* **25**, 457–466.
Iacovache, I., van der Goot, F. G. & Pernot, L. (2008). *Biochim. Biophys. Acta*, **1778**, 1611–1623.
Jancarik, J., Scott, W. G., Milligan, D. L., Koshland, D. E. Jr & Kim, S.-H. (1991). *J. Mol. Biol.* **221**, 31–34.
Lesieur, C., Frutiger, S., Hughes, G., Kellner, R., Pattus, F. & van der Goot, F. G. (1999). *J. Biol. Chem.* **274**, 36722–36728.
Leslie, A. G. W. (2006). *Acta Cryst.* D**62**, 48–57.
Matthews, B. W. (1968). *J. Mol. Biol.* **33**, 491–497.
Moniatte, M., van der Goot, F. G., Buckley, J. T., Pattus, F. & Van Dorsselaer, A. (1996). *FEBS Lett.* **384**, 269–272.
Parker, M. W., Buckley, J. T., Postma, J. P. M., Tucker, A. D., Leonard, K., Pattus, F. & Tsernoglou, D. (1994). *Nature (London)*, **367**, 292–295.
Parker, M. W. & Feil, S. C. (2005). *Prog. Biophys. Mol. Biol.* **88**, 91–142.
Rossjohn, J., Raja, S. M., Nelson, K. L., Feil, S. C., van der Goot, F. G., Parker, M. W. & Buckley, J. T. (1998). *Biochemistry*, **37**, 741–746.
Sellman, B. R. & Tweten, R. K. (1997). *Mol. Microbiol.* **25**, 429–440.
Tsitrin, Y., Morton, C. J., El Bez, C., Paumard, P., Velluz, M. C., Adrian, M., Dubochet, J., Parker, M. W., Lanzavecchia, S. & van der Goot, F. G. (2002). *Nature Struct. Biol.* **9**, 729–733.
Wilmsen, H. U., Buckley, J. T. & Pattus, F. (1991). *Mol. Microbiol.* **5**, 2745–2751.